EFFECTIVE MgO /ALUMINA / ITO NANO HETEROSTRUCTURE AS SMART MATERIAL FOR LIGHT-EMITTING DIODE

NANOHETEROESTRUCTURA EFICAZ DE MgO/ALÚMINA/ITO COMO MATERIAL INTELIGENTE PARA DIODOS EMISORES DE LUZ

Zehraa N. Abdul-Ameer

University of Baghdad, College of Science, Remote Sensing & GIS dept. Baghdad, Al jaddiryiah, 00964, Iraq.

(Recibido: 09/2022. Aceptado: 05/2023)

Abstract

Transparent conducting oxides (TCO) offer the uncommon functional combination of being both transparent and electrically conductive. For this reason, this study is concerned with the preparation of the triple heterojunction consisting of magnesium oxide, alumina, and ITO using a pulsed laser deposition method with a laser intensity of 3 J. Alumina bulk pellets in propanol were irradiated (Nd:YAG) at a wavelength of 1064 nm. Laser ablation was performed at a laser intensity of 3 J and deposited on ITO, which was then left to dry for 24 hours. The same method was used to attain magnesium nanoparticles, which were spin-coated on the previous sample and dried in a 500 °C oven for 4 hours. Then the properties of nanoparticles were investigated using X-ray diffraction, UV spectroscopy, and scanning electron microscopy (SEM). The results were obtained by UV and XRD analyses. From SEM images, the average size of the synthesized nanoparticles was determined to be about 25–35 nm. Aluminum oxide, MgO, and ITO are 1-D nanostructured semiconductors that function as transparent conducting oxide thin film while

zehraa.najim@sc.uobaghdad.edu.iq doi: https://doi.org./10.15446/mo.n67.104960

also increasing absorption in the visible spectrum. ITO is identified as an appropriate electrode material for infrared photoelectric devices.

Keywords: magnesium oxide, nanoparticles, indium tin oxide, alumina, light-emitting diode.

Resumen

Los óxidos conductores transparentes (TCO, por sus siglas en inglés) poseen la combinación funcional poco frecuente de ser transparentes y conductores de la electricidad. Por este motivo, este estudio se centra en la preparación de la heterounión triple formada por óxido de magnesio, alúmina e ITO utilizando un método de deposición por láser pulsado con una intensidad de láser de 3 J. Se irradiaron gránulos de alúmina en propanol (Nd:YAG) a una longitud de onda de 1064 nm. La ablación por láser se realizó a una intensidad de 3 J y se depositó sobre ITO, que se dejó secar durante 24 horas. Se utilizó el mismo método para obtener nanopartículas de magnesio, que se recubrieron por rotación sobre la muestra anterior y se secaron en un horno a 500 °C durante 4 horas. Posteriormente, se investigaron las propiedades de las nanopartículas mediante difracción de rayos X, espectroscopia UV y microscopia electrónica de barrido (SEM, por sus siglas en inglés). Los resultados se obtuvieron mediante análisis UV y difracción de rayos X. A partir de las imágenes de SEM, se determinó que el tamaño medio de las nanopartículas sintetizadas era de unos 25-35 nm. El óxido de aluminio, el MgO y el ITO son semiconductores 1-D nanoestructurados que funcionan como películas finas de óxido conductor transparentes al tiempo que aumentan la absorción en el espectro visible. El ITO se identifica como un material de electrodo apropiado para dispositivos fotoeléctricos infrarrojos.

Palabras clave: óxido de magnesio, nanopartículas, óxido de indio y estaño, alúmina, diodo emisor de luz.

Introduction

A variety of optoelectronic devices, including diodes, solar cells, and panel displays, among others, increasingly depend on transparent conductive materials (TCMs) as functional components [1–3]. ITO, an indium-doped oxide, has garnered significant attention as one of the transparent conducting oxides in recent times. The combination of MgO, alumina, and ITO results in a heterojunction with high electrical conductivity and transparency. In order to increase the conductivity of the alumina, because of its large surface area, it is possible to increase the number of immobilized species, resulting in better electron efficiency and hence, higher hybrid device efficiency. The n-type (ITO) has a wide energy gap, approximately 3.5–3.75 eV. It also has high conductivity, low resistance, and the ability to dope or mix with different metals to alter its surface. Alumina nanoparticles have attracted researchersínterest due to their potential applications in various fields, including optoelectronics [1].

The influence of magnesium addition on the mechanical, physical, thermal, chemical, and microstructural characteristics of the cores was examined by fabricating MgO-containing alumina-based ceramic cores using $MgTi_2O_5$ [2]. Metal oxide-loaded alumina nanoparticles that included 12.5 % ZnO and 12.5 % MgO significantly increased the effectiveness of oxidative desulfurization. The homemade Nano catalyst was characterized by applying the precipitation technique to the surface area of the Nano alumina analyzer and N_2 adsorption [3]. Magnesium oxide nanoparticles were synthesized using the chemical bath method in a range of concentrations, exploring their effect on morphologies, particle size, and energy gap in the fabrication of a UV detector [4].

Using the pulsed laser deposition method, this study investigates the fabrication of triple heterojunctions composed of magnesium oxide, alumina, and ITO. Photoluminescence spectroscopy was employed to study the optical properties of these samples, as the defect level created is significantly lower than the bottom of the conduction band. The origin of the native donor in ITO demonstrates that an oxygen vacancy cannot function

as a native donor. These combined characteristics make them suitable for various applications, including photoelectric devices. Aluminum oxide, MgO, and ITO combine the properties of a transparent conducting oxide as thin films with a one-dimensional nanostructured semiconductor, enhancing their ability to absorb visible light. ITO is particularly well-suited as an electrode material for near-infrared photoelectric devices.

Materials and Methods:

An aluminum pellet with a purity of 99.9 %, a diameter of 15 mm, and a thickness of 5 mm was placed in a vessel containing approximately 10 ml of deionized water until the water level reached about 5 mm above the target. Laser ablation was carried out using an Nd:YAG laser with a wavelength (λ) of 1064 nm, and the laser intensity used was 3 J, as depicted in the Figure 1a.

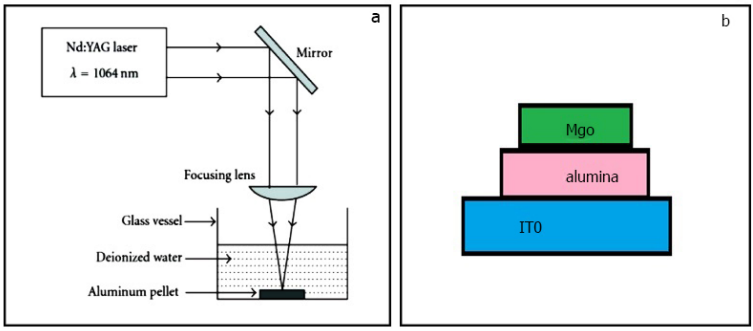

FIGURE 1. *a. Laser ablation system; b. Deposited layers array.*

A 50 mm focal-length lens was used to focus the laser beam onto the metal pellet. A total of 5,000 pulses were applied to ablate the aluminum metal target, taking approximately 40 minutes. This process yielded Al2O3 particles suspended in deionized water.

The resulting liquid sample was then applied onto ITO and dried in a 40 °C oven for 4 hours. Next, the Mg bulk pellet in propanol underwent laser irradiation to produce magnesium oxide nanoparticles. The synthesized magnesium nanoparticles were then

spin-coated onto the previously prepared film and subjected to a 500 °C oven for hours, as illustrated in the Figure 1b. The structure and morphology of the dried particle samples were investigated [5].

Results and Discussion

The X-ray diffraction spectrum in the Figure 2a depicts the XRD patterns of the synthesized MgO nanoparticles. The XRD result obtained is in agreement with the JCPDS file: 45-09456, where CuKα radiation was used for XRD studies in the 20–80° range. In the Figure 2a, the XRD analyses of MgO nanoparticles are clearly presented, displaying peaks at angles of 36.96°, 42.98°, 62.36°, 74.71°, and 78.66°, corresponding to the (0 0 2), (1 0 1), (1 0 3), (0 0 4), and (2 0 2) planes, respectively (JCPDS No. 45-09456). The XRD pattern indicates the absence of any additional impurity phases. The grain size was calculated using Scherer's equation. The diffraction phases of the MgO nanoparticles reveal the presence of the cubic phase with a crystallite size of 20 nm.

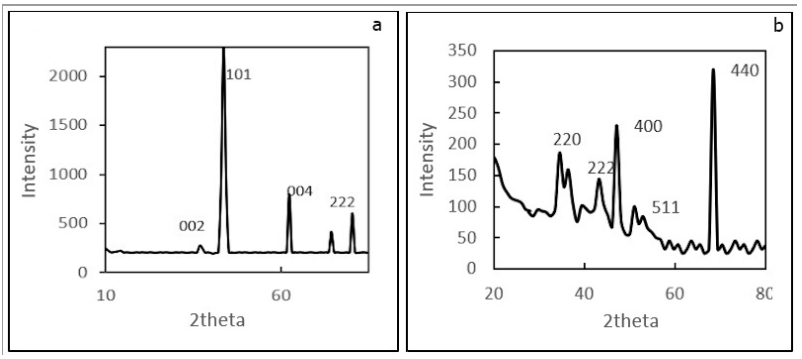

FIGURE 2. *XRD for a. MgO nanoparticles; b. alumina nanoparticles.*

$$D = 0.9\lambda/\beta cos\theta \quad \ldots\ldots\ldots \quad [1][4]$$

This equation is used to calculate nano crystallite size (D) by using XR radiation of wavelength λ (1.5 A). β is the FWHM in radians, as shown in the table (1).

The XRD pattern, which shows a high intensity (1 0 1) orientation peak, reveals the produced crystalline materials. Using (1 0 1) reflection, the mean crystallite size is determined to be 20.1 nm.

Figure 2b depicts the XRD patterns of the Al target and particles generated with 3J laser energy. The peaks at 38.49°, 46.71°, 56.76°, 61.37°, and 67.94° correspond to the typical reflection of the (220), (222), (400), (511) and (440) planes of the crystalline Al_2O_3 structure, which is correctly matched to JCPDS card no. 02-1420. According to Table 1, the average grain size of the Al_2O_3 NPs is 17.0 nm.

Parameter	**MgO Nanoparticles**	**Alumina Nanoparticles**
hkl	(002), (101), (004), (222)	(220), (222), (400),(511), (440)
β(rad)	0.013	0.017
D(nm)	20.1	17.0
ε ($*10^{-3}$lines^{-2}m^{-4})	172.5	200.25
$\delta(*10^{15}$ lines^{-2} /m^4)	1.14	1.3

TABLE 1. *XRD parameters for the synthesized specimens.*

Where ε is strain, and δ is dislocation density.

The optical band gap (Eg) of the thin film was determined using the Tauc equation:

$$(\alpha h\nu)^2 = A(h\upsilon - Eg)^n \quad \text{..... [2]}$$

Figure 3a demonstrates that the direct energy gap of MgO nanoparticles is 4.15 eV, significantly smaller than the band gap of bulk MgO (7.8 eV). Consequently, the band gap energies of the MgO nanocrystallites are lower than those of the bulk material. The nanoscale size of MgO leads to a red shift in its spectra due to the effects of quantum confinement, as evidenced by the decline in band gap values.

To investigate the optical behavior of alumina nanoparticles and their nanocomposites and obtain crucial information about their absorbance and band gaps, a study was conducted. The band gap

of the alumina nanoparticles was found to be 2.25 eV, as shown in the Figure 3b. This narrowing of the band gap is likely attributed to the significant surface area-to-volume ratio of the crystallites [6].

The energy gap of MgO/Alumina/ITO was determined, revealing that most semiconductors have an energy gap ranging from 1 to 1.5 eV, as depicted in the Figure 3c. However, a few others possess a wider band gap between 2 and 4 eV, positioning their electronic and optical properties between insulators and semiconductors. These semiconductors are used in LEDs, lasers, and radio frequency applications at much higher voltages, frequencies, and temperatures [6][7].

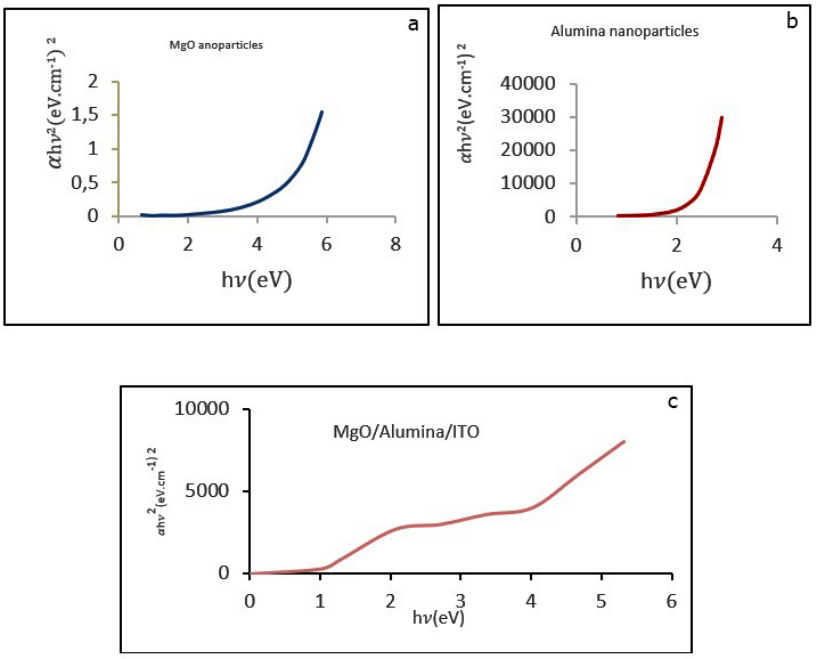

FIGURE 3. *Energy gap for a. MgO; b. alumina; c. MgO /Alumina/ITO.*

The optoelectronic characteristics of semiconductors and other materials are often evaluated through photoluminescence. The principle is straightforward: a laser with energy exceeding the material's band gap excites electrons from the valence band to the conduction band, and the material's response can be measured in

terms of the relationship between intensity and wavelength [7]. In the case of MgO nanoparticles, the presence of oxygen vacancies containing 3-coordinated, low-coordinate oxygen anions can lead to the largest fluorescence emission peak at approximately 420 nm (3.30 eV) in the violet region [8].

Photoluminescence (PL) measurements of alumina indicate the presence of a blue PL band with a wavelength of 500 nm, as green light emission. Singly ionized oxygen vacancies (F+ centers) in porous alumina membranes give rise to this band. There are other theories as to why the PL band's intensity and peak location shift as the heat-treatment temperature rises Figure 4.

The synthesized MgO/Alumina/ITO nano heterostructure exhibited photoluminescence emission at 460 nm, falling within the violet-blue range, as shown in the Figure 4. The introduction of magnesium oxide resulted in a red shift in the PL spectrum of the synthesized nano heterostructure. Cracking processes can lead to bond-breaking, nuclear motion, and the release of atoms and ions from lattice sites, thus contributing to the formation of defects [9][10]. These defects contribute to the existence of porous membranes in alumina. Additionally, the high transmittance of ITO further supports the potential use of the MgO/Alumina/ITO nano heterostructure in optoelectronic devices. Its tunable photoluminescence spanning the visible spectrum (violet-blue) makes it an attractive candidate for such applications.

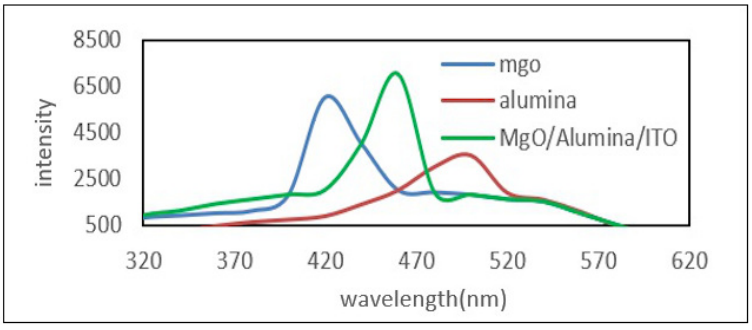

FIGURE 4. *Photoluminescence for MgO-Alumina-ITO.*

SEM images in the Figure 5 a and b depict alumina nanoparticles and the agglomeration of particles forming distinct nano flowers with a diameter of 25-50 nm. The images showcase horizontally oriented and separate nanoparticles, with a larger diameter of approximately 35 nm, and a significant presence of growing pores. Higher concentrations result in porous structures and open spaces. Upon calcination, the alumina nanoparticles exhibit a porous and spongy crystal structure, with regular pore shapes and sufficient volume for surface reactions. The evaporation of ethanol during the synthesis process may explain the observed low bulk density and wide pores in the generated nano-alumina, as evident in the SEM images.

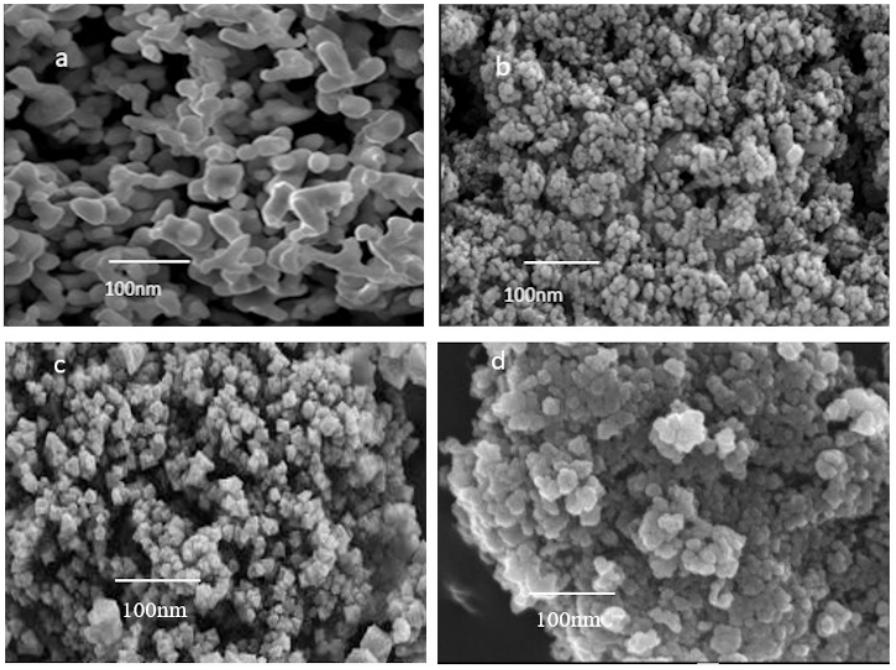

FIGURE 5. *SEM images a. Alumina; b. Alumina nano flowers; c. ITO; d. MgO/Alumina/ITO.*

As depicted in the Figure 6, the current-voltage characteristics of the MgO/alumina/ITO heterojunction device exhibit changes when exposed to light. The reverse current increases due to photocurrent

generation. The I-V characteristics are represented in two parts: the right portion represents the I-V characteristics under illumination with forward bias, while the left portion represents the reverse bias part, showcasing the I-V characteristics in the dark. However, the curve exhibits behavior consistent with that of a photodiode or light-emitting diode [11].

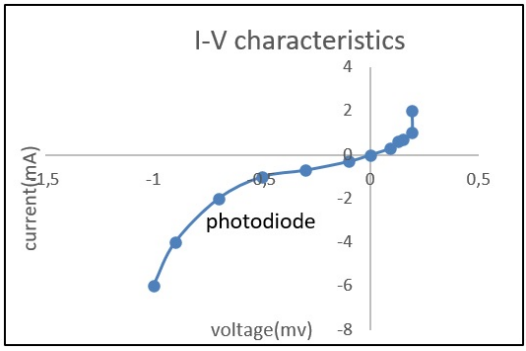

FIGURE 6. *Current-voltage characteristics of MgO/Alumina/ITO.*

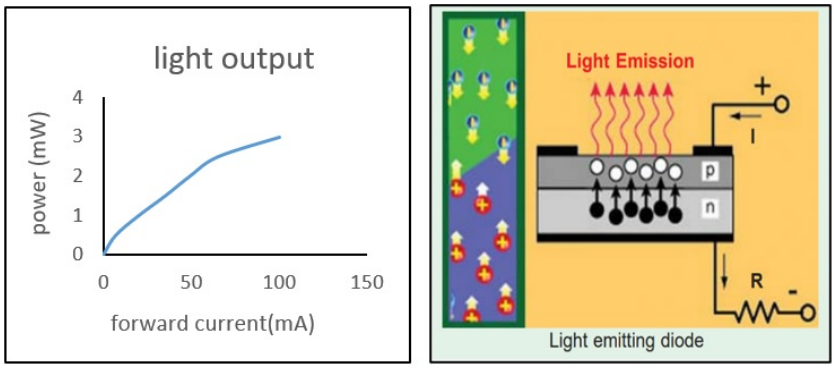

FIGURE 7. *Light-emitting diode characteristics for heterojunction MgO/Alumina/ITO.*

When powered, the forward-biased P-N junction exhibits the generation of visible light. This phenomenon occurs when electrons from the N-side traverse the junction and recombine with holes on the P-side, a process known as charge carrier recombination. Figure 7 provides an illustration of the light output resulting from this process. In order to evaluate the suitability of MgO, Alumina,

and ITO for use in light-emitting diodes (LEDs), we conducted a study on their diode behavior at room temperature. Our findings demonstrated their ability to function as current rectifiers, thereby confirming their potential for diode and LED applications as highly transparent p–n junctions [11][4].

Conclusions

In summary, we present the manufacture and characterization of MgO/Alumina/ITO heterojunction-based LEDs. The effects of n-MgO and p-Alumina on the structural, electrical, and optical characteristics of n-ITO heterostructures were examined. XRD, UV spectroscopy, and scanning electron microscopy were used to explore the characteristics of nanoparticles (SEM). The creation of nanoparticles was validated by the results of UV and XRD investigations. The average size of the produced nanoparticles was also determined to be around 25–35 nm based on the SEM picture. This one-of-a-kind combination of characteristics makes them suitable for a wide range of applications, including photoelectric devices. Aluminum oxide, MgO, and ITO combine the properties of both transparent and electrically conductive oxides as they increase absorption in the visible spectrum. For UV-Blue photoelectric devices, ITO is an appropriate electrode material.

Acknowledgement

I am grateful to the Ministry of Science and Technology for their support.

References

[1] H. Ohta and H. Hosono, Mater. Today **7**, 42 (2004).

[2] S. Shabani, R. Naghizadeh, and et al, J. Sol-Gel Sci. Techn. **96**, 539 (2020).

[3] L. Abdulateef, A. Nawaf, Q. Mahmood, O. Dahham, N. Noriman, and Z. Shayfull, AIP Conf. Proc. **2030** (2018).

[4] Z. Abdul-Ameer, Adv. nat. appl. sci. **12**, 72 (2016).

[5] T. Phuoc, B. Howard, D. Martello, Y. Soong, and M. Chyu, Opt. Lasers Eng. **46**, 829 (2008).

[6] K. Ellmer, Nat. Photonics. **6**, 809 (2012).

[7] D. Seo, J. Shim, and et al, Opt. Express **20**, 991 (2012).

[8] X. Li, Y. Yuan, and et al, J. Phys.: Condens. Matter **30**, 194002 (2018).

[9] A. N. Mohamed, J. Pure Sci. **4**, 94 (2017).

[10] T. Duong, T. Nguyen, and et al, J. Chem. **2019**, 4376429 (2019).

[11] G. Buehler, D. Thoelmann, and C. Feldmann, Adv. Mat. **19**, 2224 (2007).